

# Low-Profile Wideband Circularly Polarized Patch Antenna Using Asymmetric Feeding

Yang-Tao Wan\*, Fu-Shun Zhang, Dan Yu, Wen-Feng Chen, and Tian Li

**Abstract**—A low-profile wideband circularly polarized aperture stacked patch (ASP) antenna without air dielectric layers is presented. The new circular ASP antenna, which is fed by two orthogonal dual-offset lines through an asymmetric crossed slot, delivers a wide bandwidth of 80% for the 10-dB return loss and similar input impedance characteristics for the two ports. Then, a novel broadband 90° hybrid feed network is employed to achieve good impedance matching, balanced power splitting and consistent 90° ( $\pm 9^\circ$ ) phase shifting across the wide operating band. The two unbalanced feed lines are connected to the respective ports of the feed network comprising a three-section Wilkinson power divider and a broadband 90° phase shifter. It is found that the proposed antenna can achieve a measured impedance bandwidth of 91.3% (2.44–6.54 GHz), measured 3-dB axial ratio (AR) bandwidth of 86.4% (2.5–6.3 GHz), and measured gain bandwidth of 60.9% from 3.2 to 6.0 GHz for the gain > 4 dBic. In addition, a comparison between the proposed wideband CP antenna and related wideband CP and ASP antennas in the literature is made.

## 1. INTRODUCTION

With the rapid development of wireless communication systems, circularly polarized (CP) antennas have gained much attention than ever. It is because they not only are capable of allowing for better mobility and weather penetration, but also alleviate multipath distortion and polarization mismatch losses between the receiving and transmitting antennas. In recent years, many microstrip CP antennas of the single-fed type are reported in the literature, such as a corner-truncated square patch with a novel coaxial feed [1], wideband CP microstrip antennas with annular-ring slot or cross-shaped slot [2–4], stacked CP microstrip antennas using a new C-type single feed or a S-shaped impedance matching network [5–7], and a broadband microstrip antenna using an artificial ground structure with rectangular unit cells [8]. However, these CP antennas have relatively narrow impedance and AR bandwidths (generally less than 10%). For microstrip antennas of the dual-fed or tri-fed type [9–11], circular polarization can be generated with the use of an external polarizer, resulting in wide impedance and AR bandwidths. A circular patch antenna, employing four sequentially rotated L-probes and a novel wideband 90° hybrid feed network, delivers 10-dB impedance and 3-dB AR bandwidths of 79% and 82%, respectively [9]. The same circular patch and feeding types, using a novel 90° broadband microstrip balun, provide a 10-dB impedance bandwidth of 71% and a 3-dB AR bandwidth of 82% [10]. A tri-fed circular patch antenna with a broadband 120° phase shifter, utilizing the metamaterial transmission line, offers a 10-dB impedance bandwidth of 55% and a 3-dB AR bandwidth of 48% [11]. However, these antennas require complicated feed arrangements, such as four proximity-coupled L-probes and a metamaterial transmission line loaded with capacitors and shunt inductors, which introduce the complexity and difficulty in manufacture process.

In this paper, a low-profile wideband circularly polarized ASP antenna is presented. Compared with the conventional ASP antennas [12, 13], the new wideband circular ASP antenna yields a lower

---

*Received 5 June 2014, Accepted 5 August 2014, Scheduled 12 August 2014*

\* Corresponding author: Yang-Tao Wan (wanyangtao@163.com).

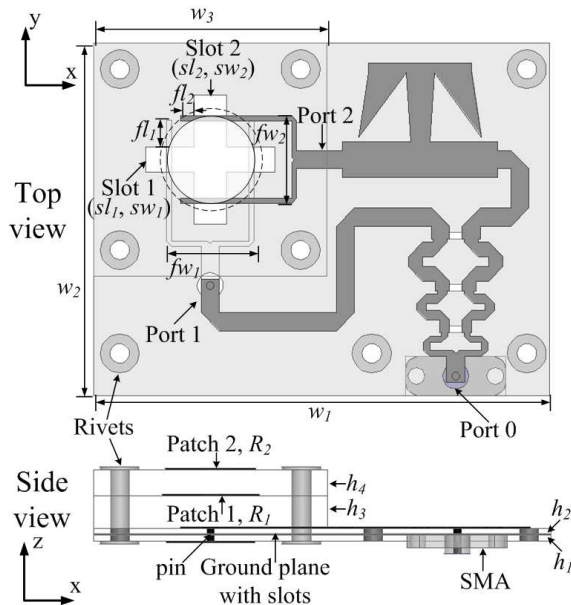
The authors are with the Science and Technology on Antenna and Microwave Laboratory, Xidian University, Xi'an 710071, P. R. China.

profile of  $0.15\lambda_0$  and a wider impedance bandwidth of 80% by employing two asymmetric feeding structures without any air/foam layers. Then, a novel broadband  $90^\circ$  hybrid feed network, comprising a broadband  $90^\circ$  phase shifter [14] and a three-section Wilkinson power divider, is introduced to achieve a wide impedance bandwidth, a good amplitude balance and a consistent  $90^\circ$  ( $\pm 9^\circ$ ) phase difference between two output ports; thus enhancing the CP performance across the whole operating frequency range. The proposed antenna exhibits a measured impedance bandwidth of 91.3% (2.44–6.54 GHz), a measured 3-dB AR bandwidth of 86.4% (2.5–6.3 GHz), and a gain bandwidth of 60.9% from 3.2 to 6.0 GHz for the gain  $> 4$  dBic. The simulation is based on the HFSS and a good agreement is observed between the simulation and measurement.

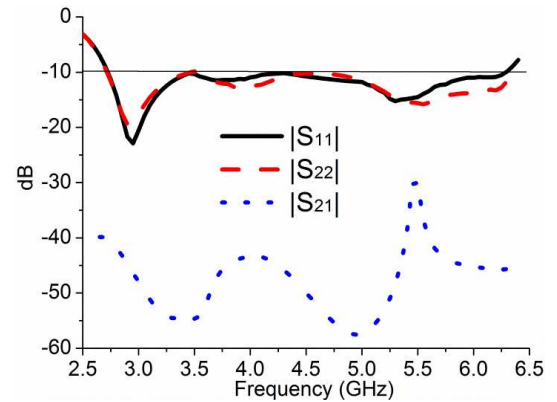
## 2. ANTENNA DESIGN

Figure 1 shows the configuration of the new ASP antenna. The proposed antenna consists of four dielectric layers using the same substrate with a relative dielectric permittivity of  $\epsilon_r = 2.65$  and a loss tangent of 0.0025. As can be seen from this diagram, two circular patches are mounted on two dielectric layers located above the feed layer with thicknesses of  $h_4$  and  $h_3$ , respectively. Two orthogonal dual-offset feed lines are printed on a separate layer with thicknesses of  $h_2$  and  $h_1$  on the opposite sides of the ground plane, respectively. Power is coupled to the patch radiators from the feed networks via a cross-shaped slot in the common ground plane. Noting that, the upper feed network (Port 2) can couple power to the circular patch elements directly, which cannot be negligible because the thick foam layer between the slot and the patches is removed for a lower profile antenna structure compared with the conventional ASP antennas. Therefore, the two orthogonal dual-offset feed lines ( $fl_1$ ,  $fw_1$ ,  $fl_2$ ,  $fw_2$ ) and the cross-shaped slot ( $sl_1$ ,  $sw_1$ ,  $sl_2$ ,  $sw_2$ ) are designed to be asymmetric to minimize the direct coupling from the upper feed line to the patches and obtain similar input impedance characteristics for both the two ports. This arrangement has the advantage of widening the impedance bandwidth of both the two ports and reducing the complexity in fabricating the proposed antenna. It is because the coupling levels between the two feed lines and the corresponding slot are controlled separately. For each port, the input impedance can be optimized to obtain a wide  $50\Omega$  impedance matching with little impact on the other port.

Figure 2 shows the simulated reflection coefficients of Port 1 and Port 2, and the isolation between



**Figure 1.** Configuration of the proposed antenna.



**Figure 2.** Simulated  $S$ -parameters of the new ASP antenna.

the two ports. As can be seen from these responses, the new ASP antenna exhibits a 10-dB impedance bandwidth of 80% (2.7–6.3 GHz) for both the ports. The coupling between the slot and the patch element for Port 2 excitation is different from that for Port 1 excitation, which leads to the slightly different reflection coefficients between the two ports as shown in Figure 2. It can also be seen that the new ASP antenna has an isolation of more than 30 dB between the two ports across the whole operating band. This is because the two feed lines are separated by the ground plane which weakens the cross coupling between them.

### 3. WIDEBAND FEED NETWORK

The proposed broadband microstrip feed network shown in Figure 3 has the advantage of providing equal amplitude and 90° phase shift across a wide bandwidth. It comprises a cascade of a three-section Wilkinson power divider and a broadband 90° phase shifter [14]. With reference to Figure 3, after the original input signal from Port 0 is split into two ways, they pass through the two paths of the 90° phase shifter respectively to obtain a stable phase shifting. The design equations for the proposed feed network structure are presented in [9] in details. The characteristic impedance  $Z_0$  of both the input and output ports of the feed network are 50 Ω.  $Z_1$ ,  $Z_2$  and  $Z_3$  stand for the characteristic impedances of the quarter wavelength microstrip lines in the power divider, respectively, and  $R_1$ ,  $R_2$  and  $R_3$  are the isolation resistances.  $Z_4$  and  $Z_5$  stand for the characteristic impedances of the main microstrip line and the open stub in the phase shifter, respectively, and  $Z_6$  stands for characteristic impedance of the reference line. For the sake of brevity, we simply present the optimized values of these parameters in this paper:  $Z_0 = 50 \Omega$ ,  $Z_1 = 55.6 \Omega$ ,  $Z_2 = 70.7 \Omega$ ,  $Z_3 = 89.9 \Omega$ ,  $R_1 = 510 \Omega$ ,  $R_2 = 180 \Omega$ ,  $R_3 = 100 \Omega$ ,  $Z_4 = 30 \Omega$ ,  $Z_5 = 45 \Omega$  and  $Z_6 = 50 \Omega$ .

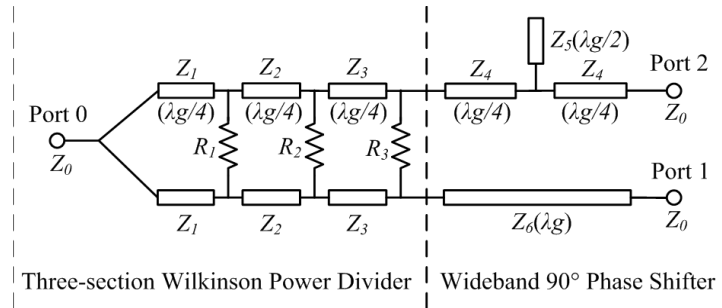


**Figure 3.** Schematic of the proposed broadband 90° hybrid feed network.

### 4. RESULTS AND DISCUSSIONS

To verify the design, a prototype of the wideband CP antenna has been fabricated and measured. Figure 4 shows photos of the prototype, the parameters of which are  $fl_1 = 4.1 \text{ mm}$ ,  $fw_1 = 13.6 \text{ mm}$ ,  $fl_2 = 2.1 \text{ mm}$ ,  $fw_2 = 13.6 \text{ mm}$ ,  $sl_1 = 20 \text{ mm}$ ,  $sw_1 = 4 \text{ mm}$ ,  $sl_2 = 20 \text{ mm}$ ,  $sw_2 = 5 \text{ mm}$ ,  $w_1 = 70.5 \text{ mm}$ ,  $w_2 = 54.5 \text{ mm}$ ,  $w_3 = 36 \text{ mm}$ ,  $h_1 = 1 \text{ mm}$ ,  $h_2 = 1 \text{ mm}$ ,  $h_3 = 5 \text{ mm}$ ,  $h_4 = 4 \text{ mm}$ ,  $R_1 = 7.5 \text{ mm}$ , and  $R_2 = 7 \text{ mm}$ . The measured and simulated reflection coefficients are depicted in Figure 5, and a reasonable agreement between them is obtained. The measured results show that the proposed antenna exhibits a measured 10-dB impedance bandwidth of 91.3% (2.44–6.54 GHz), which is little smaller than the simulated result of 92.7% (2.36–6.44 GHz) due possibly to the inaccuracies in the fabrication process. Figure 6 shows the measured and simulated ARs of the proposed wideband antenna at  $\theta = 0^\circ$ . With reference to the figure, the simulated and measured 3-dB AR bandwidths are 90.3% (2.4–6.35 GHz) and 86.4% (2.5–6.3 GHz), respectively. It is worth mentioning that the measured AR pass band completely falls within the measured impedance pass band, indicating that the entire AR bandwidth of 86.4% (2.5–6.3 GHz) is usable.

Figure 7 shows the measured and simulated radiation patterns in the  $X$ - $Z$  and  $Y$ - $Z$  planes at three different frequencies of 3.0, 4.5, and 6.0 GHz, respectively. It is clearly seen that the proposed

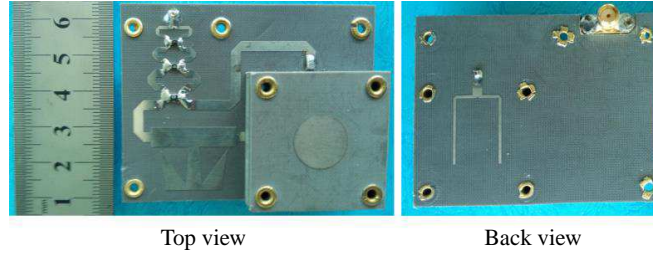


Figure 4. Photograph of the prototype antenna.

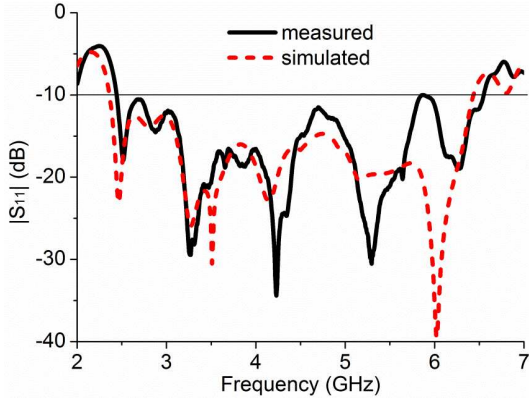


Figure 5. Measured and simulated  $|S_{11}|$  of the proposed antenna.

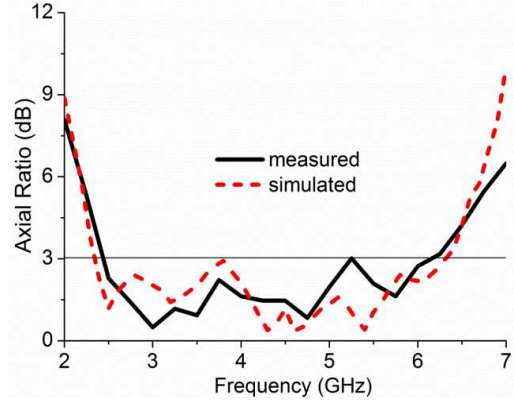


Figure 6. Measured and simulated ARs of the proposed antenna.

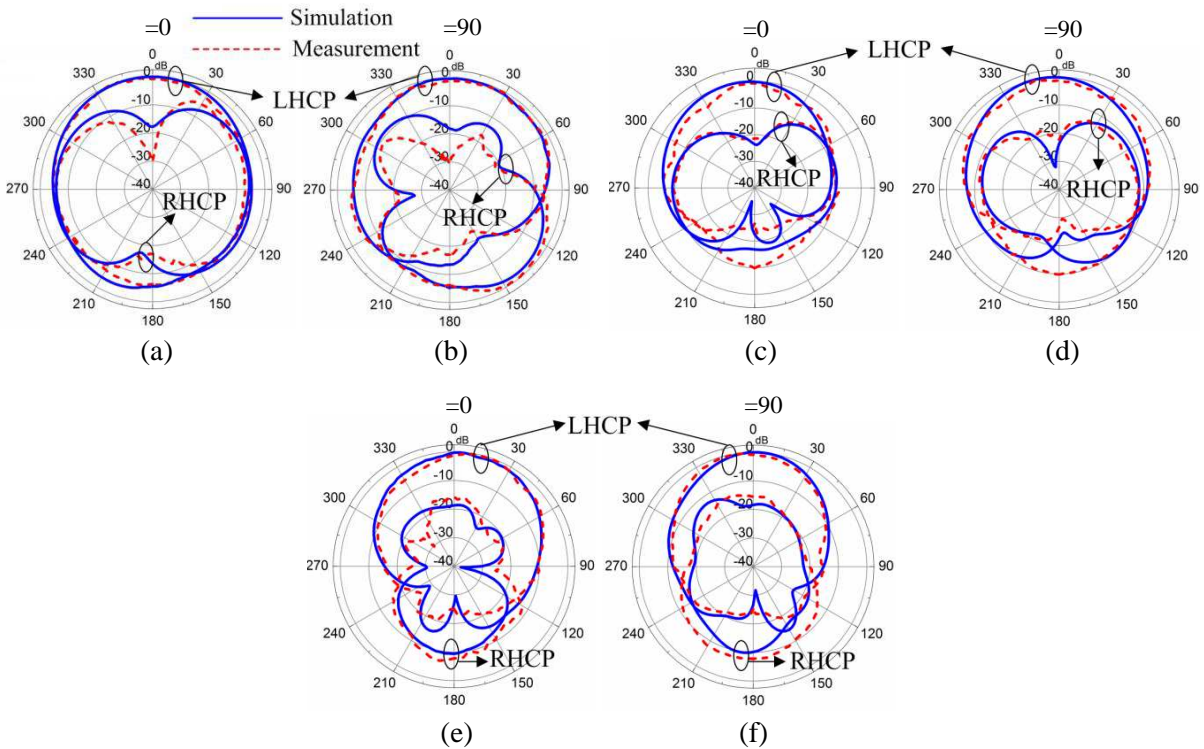
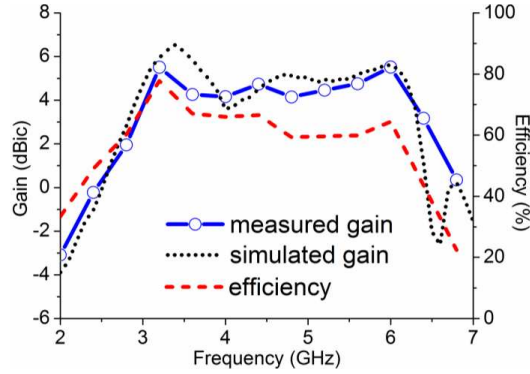


Figure 7. Simulated and measured radiation patterns in the (a), (c), (e) X-Z ( $\varphi = 0^\circ$ ) and (b), (d), (f) Y-Z ( $\varphi = 90^\circ$ ) planes at (a), (b) 3 GHz, (c), (d) 4.5 GHz, and (e), (f) 6 GHz.



**Figure 8.** Measured and simulated gains at  $\theta = 0^\circ$ , along with the measured efficiencies of the prototype antenna.

**Table 1.** Comparison of various wideband CP and ASP antennas.

Referenced antenna	10-dB impedance bandwidth	3-dB AR bandwidth	Gain bandwidth	Dimension ( $\lambda_0$ at center frequency)	Feed method
[9]	79.4%	82%	56.1% ( $> 3$ dBic)	$1.7 \times 1.7 \times 0.18$	L-probes with air substrate
[10]	71.3%	81.6%	52.2% ( $> 3$ dBic)	$1.7 \times 1.7 \times 0.16$	L-probes with air substrate
[11]	54.8%	47.9%	40% ( $> 3$ dBic)	$1.0 \times 1.0 \times 0.17$	Three-fed with air gap
[12]	52%	-	50% ( $> 5$ dBic)	$0.7 \times 0.7 \times 0.18$	Slot-coupled with air gap
[13]	40%	-	40% ( $> 7$ dBic)	$0.5 \times 0.5 \times 0.22$	Slot-coupled with foam gap
Proposed antenna	91.3%	86.4%	60.9% ( $> 4$ dBic)	$1.0 \times 0.8 \times 0.15$	Slot-coupled without air gap

antenna radiates a left-hand circular polarization (LHCP) wave in the broadside direction ( $\theta = 0^\circ$ ). The measured radiation patterns are not very symmetrical with respect to the  $Z$ -direction due to the asymmetry of the feeding network and the ground plane. In the boresight direction ( $\theta = 0^\circ$ ), the co-polarized (LHCP) field is at least 15 dB stronger than the corresponding cross-polarized (RHCP) counterpart, showing good polarization purity of the CP field. Figure 8 shows the measured and simulated antenna gains at  $\theta = 0^\circ$ , along with the measured radiation efficiencies of the proposed CP antenna. With reference to the figure, the CP circular patch antenna exhibits a measured gain bandwidth of 60.9% from 3.2 to 6.0 GHz for the LHCP gain  $> 4$  dBic. It is also observed that the peak gain of the antenna is about 5.6 dBic at 3.2 GHz in the broadside direction and the measured gain values are smaller than the simulated ones, which is caused by the cable’s transmission loss in the far-field measurements of the proposed antenna. By observing the radiation efficiency of the proposed antenna in Figure 8, it is believed that the measured gain bandwidth is smaller than the impedance bandwidth due to the low radiation efficiency at the spectral edge frequency which is caused by the isolation resistances.

### 5. COMPARISON

The related wideband CP antennas [9–11] and the conventional ASP antennas [12, 13] are listed in Table 1. Compared with the wideband CP antennas [9–11], the proposed wideband CP antenna has the widest impedance, AR and gain bandwidths. Notably, the proposed CP antenna has the lowest

profile of  $0.15\lambda_0$  at the center frequency because the antenna is fabricated without any air substrates. Moreover, the antennas with air layers will introduce the complexity and difficulty in manufacture process. Furthermore, although the conventional ASP antennas [13, 14] have a smaller cross section, they are higher in profile and narrower in impedance bandwidth. The comprehensive comparison leads to the conclusion that the proposed wideband CP antenna has the widest impedance and AR bandwidths with a low-profile and simple antenna structure.

## 6. CONCLUSION

In this paper, a low-profile wideband CP ASP antenna using an asymmetry feeding structure is presented. Compared with the conventional ASP antennas, the new wideband circular ASP antenna yields a lower profile of  $0.15\lambda_0$ , a wider impedance bandwidth of 91%, a lower fabrication cost, and a simple antenna structure without any air/foam layers. By introducing a novel broadband  $90^\circ$  hybrid feed network, the proposed antenna exhibits a measured impedance bandwidth of 91.3% (2.44–6.54 GHz), measured 3-dB AR bandwidth of 86.4% (2.5–6.3 GHz), and measured gain bandwidth of 60.9% from 3.2 to 6.0 GHz for the gain  $> 4$  dBic. Good agreement is also observed between simulation and measurement. Therefore, the proposed antenna with a good wideband CP performance is suitable for wireless communication applications.

## REFERENCES

1. Chang, F. S., K. L. Wong, and T. W. Chiou, "Low-cost broadband circularly polarized patch antenna," *IEEE Trans. Antennas Propag.*, Vol. 51, No. 10, 3006–3009, Oct. 2003.
2. Su, C. W. and J. S. Row, "Slot-coupled microstrip antenna for broadband circular polarization," *Electron. Lett.*, Vol. 42, No. 6, 318–319, Mar. 2006.
3. Guo, Y. X., L. Bian, and X. Q. Shi, "Broadband circularly polarized annular-ring microstrip antenna," *IEEE Trans. Antennas Propag.*, Vol. 57, No. 8, 2471–2477, Aug. 2009.
4. Nasimuddin, Z. N. Chen, and X. M. Qing, "A compact circularly polarized cross-shaped slotted microstrip antenna," *IEEE Trans. Antennas Propag.*, Vol. 60, No. 3, 1584–1588, Mar. 2012.
5. Nasimuddin, K. P. Esselle, and A. K. Verma, "Wideband circularly polarized stacked microstrip antennas," *IEEE Antennas Wireless Propag. Lett.*, Vol. 6, 21–24, 2007.
6. Wu, T. Q., H. Su, L. Y. Gan, H. Z. Chen, J. Y. Huang, and H. W. Zhang, "A compact and broadband microstrip stacked patch antenna with circular polarization for 2.45-GHz mobile RFID reader," *IEEE Antennas Wireless Propag. Lett.*, Vol. 12, 623–626, 2013.
7. Shekhawat, S., P. Sekra, D. Bhatnagar, V. K. Saxena, and J. S. Saini, "Stacked arrangement of rectangular microstrip patches for circularly polarized broadband performance," *IEEE Antennas Wireless Propag. Lett.*, Vol. 9, 910–913, 2010.
8. Nakamura, T. and T. Fukusako, "Broadband design of circularly polarized microstrip patch antenna using artificial ground structure with rectangular unit cells," *IEEE Trans. Antennas Propag.*, Vol. 59, No. 6, 2103–2110, Jun. 2011.
9. Bian, L., Y. X. Guo, L. C. Ong, and X. Q. Shi, "Wideband circularly polarized patch antenna," *IEEE Trans. Antennas Propag.*, Vol. 54, No. 9, 2682–2686, Sep. 2006.
10. Guo, Y. X., K. W. Khoo, and L. C. Ong, "Wideband circularly polarized patch antenna," *IEEE Trans. Antennas Propag.*, Vol. 56, No. 2, 319–326, Feb. 2008.
11. Lin, C., F. S. Zhang, Y. C. Jiao, F. Zhang, and X. Xue, "A three-fed microstrip antenna for wideband circular polarization," *IEEE Antennas Wireless Propag. Lett.*, Vol. 9, 359–362, 2010.
12. Ghorbani, K. and R. B. Waterhouse, "Dual polarized wide-band aperture stacked patch antennas," *IEEE Trans. Antennas Propag.*, Vol. 52, No. 8, 2171–2174, Aug. 2004.
13. Serra, A. A., P. Nepa, G. Manara, G. Tribellini, and S. Cioci, "A wide-band dual polarized stacked patch antenna," *IEEE Antennas Wireless Propag. Lett.*, Vol. 6, 141–143, 2007.
14. Zheng, S. Y., W. S. Chan, and K. F. Man, "Broadband phase shifter using loaded transmission line," *IEEE Microw. Wireless Comp. Lett.*, Vol. 20, No. 9, 498–500, Sep. 2010.